MICROSCOPIC INSIGHT OF MOLECULARLY IMPRINTED SOL-GEL MATRIX FOR CREATININE-RECOGNISED BIOSENSOR

ANG QIAN YEE

UNIVERSITI SAINS MALAYSIA

2018

MICROSCOPIC INSIGHT OF MOLECULARLY IMPRINTED SOL-GEL MATRIX FOR CREATININE-RECOGNISED BIOSENSOR

by

ANG QIAN YEE

Thesis submitted in fulfillment of the
requirements for the degree of
Doctor of Philosophy

September 2018

ACKNOWLEDGEMENT

My foremost appreciation goes to Assoc. Prof. Dr. Low Siew Chun for her supervision throughout the entire study. Without her valuable commentaries, insightful technical feedback and knowledge as well as her continuous encouragement, this study would not have been possible to achieve the completion. Furthermore, I am grateful that she has given me very much academic freedom to explore my ideas in this study while constantly keeping me on track. Her selfless advice and sharing in person have enlightened me a lot for my future endeavours.

Besides, I am blessed to have the technical assistance and cooperation from all the administrative and technical staffs of School of Chemical Engineering. Their technical support in this project is very much indeed. I would like to extend my acknowledgement to the financial support from the Ministry of Higher Education of Malaysia and Universiti Malaysia Perlis for the past three years. The full funding provided by the Ministry of Science, Technology and Innovation (MOSTI) in this research through ScienceFund (Grant No.: 305/PJKIMIA/6013393) are gratefully acknowledged too.

Deepest appreciation to my family and friends for their patience in providing me unfailing moral support to confront the ups and downs throughout my study. As well, I wish to express my gratitude to those who had offered their kindness along this research journey.

Ang Qian Yee
September 2018

TABLE OF CONTENTS

	Page
ACKNOWLEDGEMENT	ii
TABLE OF CONTENTS	iii
LIST OF TABLES	viii
LIST OF FIGURES	xi
LIST OF PLATES	xv
LIST OF ABBREVATIONS	xvi
LIST OF SYMBOLS	xviii
ABSTRAK	xxi
ABSTRACT	xxiv
CHAPTER ONE: INTRODUCTION	
1.1 Molecularly Imprinted Polymer (MIP)	1
1.2 Sol-Gel Approach	5
1.3 Creatinine	7
1.4 Problem Statement	8
1.5 Research Objectives	10
1.6 Scope of Study	11
1.7 Thesis Organisation	13
CHAPTER TWO: LITERATURE REVIEW	
2.1 Molecular Imprinting Technology	15
2.1.1 Molecular Imprinting Principle	15

2.1.2 Molecular Imprinting Technique 17

2.1.2(a) Bulk Polymerisation 17

2.1.2(b) Free-Radical Polymerisation 19

2.1.2(c) Sol-Gel Polymerisation 20

2.2 Formulation on Cre-MIP Synthesis 21

2.2.1 Cross-linker 22

2.2.2 Monomer 24

2.2.3 Eluent Used for Template Removal 28

2.3 Molecular Modelling of MIP 29

2.3.1 Semi-Empirical Method 30

2.4 Potential of MIP in Biomedical Diagnostics 32

2.5 Development of Biosensor in Biomedical Diagnostics 33

2.5.1 MIP-Based Optical Sensing 34

2.5.2 MIP-Based Electrochemical Sensing 37

2.6 Research Gap 43

CHAPTER THREE: MATERIALS AND METHODS

3.1 Research Flowchart 45

3.2 Raw Materials and Chemicals 46

3.3 Synthesis of MIP 47

3.3.1 Selection of Cross-Linker 49

3.3.2 Effect of Cross-Linking Density 49

3.3.3 Effect of Porosity Factor 50

3.3.4 Morphological Characterisation of MIP 50

3.3.4(a) Fourier Transform Infrared Spectroscopy (FTIR) 50

3.3.4(b) Thermal Gravimetric Analysis (TGA) 51

3.3.4(c) Field Emission Scanning Electron Microscope (FESEM) 51

3.3.4(d) Nitrogen Adsorption-Desorption Analysis 51

3.3.4(e) Energy Dispersive Spectroscopy (EDS) 52

3.4 Adsorption Study 52

3.4.1 Equilibrium Analysis 53

3.4.2 Kinetics Analysis 54

3.4.3 Isotherm Analysis 55

3.4.3(a) Langmuir Isotherm 55

3.4.3(b) Freundlich Isotherm 56

3.4.3(c) Temkin Isotherm 57

3.4.3(d) Dubinin-Radushkevich Isotherm 57

3.4.4 Mass Transfer Analysis 58

3.4.4(a) Diffusion Analysis 58

3.4.4(b) Scatchard Analysis 59

3.4.5 Thermodynamic Analysis 60

3.5 Rigidity Assessment of MIP 61

3.5.1 Elution Effect 61

3.5.2 Solvation Analysis 61

3.6 Morphological Modelling of Cre-MIP 62

3.6.1 Geometry Optimisation and Energy Calculation 62

3.7 Selectivity Study 63

3.7.1 Ideal Selectivity 64

3.7.2 Binary Selectivity 65

3.8 Development of Cre-MIP Biosensor 65

3.8.1 Cre-MIP-Coated Electrode 65

3.8.1(a) Preparation of Cre-MIP-Coated Electrode 65

3.8.1(b) Sensing Performance of Cre-MIP-Coated Electrode 66

3.8.2 Cre-MIP Film Electrode 66

3.8.2(a) Preparation of Cre-MIP Film Electrode 66

3.8.2(b) Sensing Performance of Cre-MIP Biosensor 66

CHAPTER FOUR: RESULTS AND DISCUSSION

4.1 Synthesis of Molecularly Imprinted Sol-Gel Matrix for Selective Recognition of Cre 69

4.1.1 Selection of Cross-Linker 71

4.1.2 Cre-Binding Mechanism on MIP 77

4.1.2(a) Affinity Attraction (Binding Factor i) 79

4.1.2(b) Porosity Factor (Binding Factor ii) 81

4.1.2(c) Shape Memory (Binding Factor iii) 83

4.1.3 Adsorption Study of MIP 85

4.1.3(a) Adsorption Kinetics of MIP 86

4.1.3(b) Adsorption Characteristics of MIP 88

4.1.3(c) Mass Transfer Properties of Cre on MIP 91

4.1.3(d) Thermodynamic Analysis of MIP 94

4.2 Shape Memory Stiffness of MIP 97

4.2.1 Elution Effect on MIP 98

4.2.2 Solvation Effect on MIP and NIP 104

4.3 Morphological Modelling by HyperChem 112

4.3.1 Geometry Optimisation of Prepolymerisation Complexes 112

4.3.2 Intermolecular Interactions of MIP by HyperChem 115

4.3.3 Recognition Properties of MIP by HyperChem 119

4.4 Selectivity Analysis of MIP 122

4.4.1 Ideal Case 123

4.4.2 Binary Case 127

4.5 Concept of Cre-MIP Biosensor 129

4.5.1 Cre-MIP-Coated Electrode 129

4.5.2 Cre-MIP Film Electrode 132

4.5.3 Electrochemical Performance of Cre-MIP Biosensor 135

CHAPTER FIVE: CONCLUSION AND RECOMMENDATION

5.1 Conclusion 140

5.2 Recommendation for Future Research 143

REFERENCES 145

APPENDICES

Appendix A: SPECTROPHOTOMETRY ANALYSIS

Appendix B: HPLC ANALYSIS

LIST OF PUBLICATIONS

LIST OF TABLES

		Page
Table 1.1	Comparison of MIP and natural biological receptor	4
Table 2.1	Comparison of Cre-based MIP with literatures.	25
Table 2.2	Optical sensing and detection of MIP in biomedical diagnostics.	35
Table 2.3	Electrochemical sensing and detection of MIP in biomedical diagnostics.	40
Table 3.1	List of chemicals used.	46
Table 4.1	Pore characteristics of Cre-adsorbed MIP_{AMPS} and MIP_{Al3+}. Note: MIP_{AMPS} and MIP_{Al3+} were synthesised using a constant molar ratio of template:cross-linker:monomer (Cre:AMPS/Al^{3+}:TEOS) at 1:5:5.	77
Table 4.2	Adsorbed amounts of Cre by MIP and NIP at different molarities of TEOS. Note: The molar ratios of template:cross-linker (Cre:Al^{3+}) were kept constant at 1:5 (MIP) and 0:5 (NIP).	82
Table 4.3	Pore characteristics of Cre-adsorbed MIP at different molarities of TEOS. Note: The molar ratios of template:cross-linker (Cre:Al^{3+}) were kept constant at 1:5.	83
Table 4.4	Contribution of shape factor ($\Delta Cre_{MIP-NIP}$).	84
Table 4.5	Elemental analyses by energy dispersive spectroscopy (EDS) of MIP and NIP. Note: MIP and NIP were synthesised using constant molar ratio of template:cross-linker:monomer (Cre:Al^{3+}:TEOS) at 1:5:5 (MIP) and 0:5:5 (NIP), respectively.	84
Table 4.6	Kinetic constants for the pseudo-first-order and pseudo-second order equations for adsorption of Cre by MIP and NIP. Note: MIP and NIP were synthesised using constant molar ratios of template:cross-linker:monomer (Cre:Al^{3+}:TEOS) at 1:5:5 and 0:5:5, respectively.	86
Table 4.7	Isotherm parameters for adsorption of Cre by MIP and NIP. Note: MIP and NIP were synthesised using constant molar ratios of template:cross-linker:monomer (Cre:Al^{3+}:TEOS) at 1:5:5 and 0:5:5, respectively.	89
Table 4.8	Pore diffusion coefficients of MIP. Note: MIP was synthesised using a constant molar ratio of template:cross-linker:monomer (Cre:Al^{3+}:TEOS) at 1:5:5.	92

Table 4.9	Affinity parameters for the Scatchard plot. Note: MIP and NIP were synthesised using constant molar ratios of template:cross-linker:monomer (Cre:Al^{3+}:TEOS) at 1:5:5 and 0:5:5, respectively.	94
Table 4.10	Thermodynamic parameters for adsorption of Cre by MIP and NIP. Note: MIP and NIP were synthesised using constant molar ratios of template:cross-linker:monomer (Cre:Al^{3+}:TEOS) at 1:5:5 and 0:5:5, respectively.	95
Table 4.11	Cre-extraction efficiencies of MIP using different eluents. Note: MIP was synthesised using a constant molar ratio of template:cross-linker:monomer (Cre:Al^{3+}:TEOS) at 1:5:5.	100
Table 4.12	Elemental analysis by energy dispersive spectroscopy (EDS) of MIP extracted using different eluents. Note: MIP was synthesised using a constant molar ratio of template:cross-linker:monomer (Cre:Al^{3+}:TEOS) at 1:5:5.	102
Table 4.13	Mass loss of MIP and NIP after extraction. Note: MIP and NIP were synthesised using constant molar ratios of template:cross-linker:monomer (Cre:Al^{3+}:TEOS) at 1:5:5 and 0:5:5, respectively.	103
Table 4.14	Pore characteristics of MIP (before and after extraction) and NIP (before extraction).	107
Table 4.15	Mulliken atomic charges of the atoms in Cre, Cr, *N*-hyd, 2-pyr, Al^{3+} and hydrolysed TEOS.	113
Table 4.16	Interaction energies (ΔE) of MIP and NIP at different molar ratios.	120
Table 4.17	Ideal selectivity coefficients (k_{Ideal}) of MIP for Cre with respect to its analogues (Cr, *N*-hyd and 2-pyr) at low (*ca.* 15 mg L^{-1}) and high concentrations (*ca.* 100 mg L^{-1}), respectively. Note: MIP was synthesised using a constant molar ratio of template:cross-linker:monomer (Cre:Al^{3+}:TEOS) at 1:5:5.	125
Table 4.18	Interaction energies (ΔE) of Cre and its analogues (Cr, *N*-hyd and 2-pyr) to MIP and change of partial charges ($\Delta\delta$) of potential functional groups of Cre and its analogues with respect to Al^{3+} and TEOS via HyperChem in vacuo.	126
Table 4.19	Competitive selectivity coefficients (k_{Binary})of MIP for Cre with respect to its analogues (Cr, *N*-hyd and 2-pyr) in binary mixture solutions. Note: MIP was synthesised using a constant molar ratio of template:cross-linker:monomer (Cre:Al^{3+}:TEOS) at 1:5:5.	129

Table 4.20 Comparison of the adsorbed amounts of Cre by MIP and NIP with additives (MTEOS and PTEOS) and without additive. Note: $MIP_{additive}$ and $NIP_{additive}$ were synthesised using constant molar ratios of template:cross-linker:monomer:additives (Cre:Al^{3+}:TEOS:MTEOS: PTEOS) at 1:5:5:0.5:0.5 and 0:5:5:0.5:0.5, respectively. MIP and NIP were synthesised using constant molar ratios of Cre:Al^{3+}:TEOS at 1:5:5 and 0:5:5, respectively. 132

Table 4.21 Ideal selectivity coefficients (k_{Ideal}) of the CE-MIP film electrode for Cre with respect to Cr at different iso-concentrations. 138

Table 4.22 The peak current variations of the CE-MIP film electrode for Cre and Cr in individual and binary mixture solutions at 0.7 V. 139

LIST OF FIGURES

		Page
Figure 1.1	Schematic illustration of molecular imprinting.	1
Figure 1.2	Schematic illustration of molecular imprinting via sol-gel process; M is a network-forming element, e.g., Si, Ti, etc.; R refers to an alkyl radical (Lee and Kunitake, 2013).	6
Figure 2.1	Schematic diagram of (A) covalent and (B) non-covalent molecular imprinting approaches (Haupt and Mosbach, 2000).	15
Figure 2.2	Free radical polymerisation of methyl methacrylate into poly(methyl methacrylate).	19
Figure 2.3	Schematic representation of MIP-based electrochemical biosensor.	38
Figure 3.1	Flowchart of the overall study.	45
Figure 3.2	Removal of the Cre template from MIP.	48
Figure 3.3	Chemical structures of (A) Cre, (B) Cr, (C) *N*-hyd and (D) 2-pyr.	63
Figure 3.4	Schematic representation of the electrochemical measurement of a Cre-based biosensor.	67
Figure 3.5	Schematic representation of the experimental set-up of analyte solution.	68
Figure 4.1	Chemical structures of (A) Cre and (B) TEOS.	70
Figure 4.2	FTIR spectra of (A) Cre, (B) TEOS, (C) MIP (before extraction) and (D) NIP (before extraction). Note: MIP and NIP were synthesised using constant molar ratios of template:cross-linker:monomer (Cre:Al^{3+}:TEOS) at 1:5:5 (MIP) and 0:5:5 (NIP), respectively.	70
Figure 4.3	TGA of MIP (after extraction), NIP (after extraction) and the polymerised TEOS. Note: MIP and NIP were synthesised using constant molar ratios of template:cross-linker:monomer (Cre:Al^{3+}:TEOS) at 1:5:5 (MIP) and 0:5:5 (NIP), respectively.	71

Figure 4.4 Comparison of the adsorbed amounts of Cre by MIP and NIP using AMPS and Al^{3+} as the cross-linkers. Note: MIP and NIP were synthesised using constant molar ratios of template:cross-linker:monomer (Cre:AMPS/Al^{3+}:TEOS) at 1:5:5 (MIP) and 0:5:5 (NIP), respectively. 73

Figure 4.5 Schematic diagram of intermolecular interactions between Cre, cross-linkers (A, AMPS and B, Al^{3+}, respectively) and TEOS in MIP. 73

Figure 4.6 Schematic diagram of the binding interaction between Cre, Al^{3+} and TEOS. Note: Yellow and red lines indicate the electron sharing between Cre–Al^{3+} and Al^{3+}–TEOS, respectively. Brown line refers to hydrogen bonding. 78

Figure 4.7 Adsorbed amounts of Cre by MIP and NIP and imprinting factors (α) at different molarities of Al^{3+}. Note: The molar ratios of template:monomer (Cre:TEOS) were kept constant at 1:5 (MIP) and 0:5 (NIP). 80

Figure 4.8 Adsorption kinetics of MIP at different concentrations. Note: MIP was synthesised using a constant molar ratio of template:cross-linker:monomer (Cre:Al^{3+}:TEOS) at 1:5:5. 85

Figure 4.9 (A) Pseudo-first-order and (B) pseudo-second-order adsorptions of Cre by MIP and NIP. Note: MIP and NIP were synthesised using constant molar ratios of template:cross-linker:monomer (Cre:Al^{3+}:TEOS) at 1:5:5 and 0:5:5, respectively. 87

Figure 4.10 (A) Langmuir, (B) Freundlich, (C) Temkin and (D) Dubinin-Radushkevich adsorption isotherms of Cre by MIP and NIP. Note: MIP and NIP were synthesised using constant molar ratios of template:cross-linker:monomer (Cre:Al^{3+}:TEOS) at 1:5:5 and 0:5:5, respectively. 88

Figure 4.11 Pore diffusion of MIP by (A) film diffusion mass transfer rate equation and (B) Dunwald–Wagner intraparticle diffusion model. Note: MIP was synthesised using a constant molar ratio of template:cross-linker:monomer (Cre:Al^{3+}:TEOS) at 1:5:5. 92

Figure 4.12 Scatchard plots of MIP and NIP. Note: MIP and NIP were synthesised using constant molar ratios of template:cross-linker:monomer (Cre:Al^{3+}:TEOS) at 1:5:5 and 0:5:5, respectively. 93

Figure 4.13 The plot of ln K_D against $1/T$ for adsorption of Cre by MIP and NIP. Note: MIP and NIP were synthesised using constant molar ratios of template:cross-linker:monomer (Cre:Al^{3+}:TEOS) at 1:5:5 and 0:5:5, respectively. 96

Figure 4.14 FTIR spectra of MIP extracted using (A) DI water, (B) methanol, (C) propanol and (D) chloroform. Note: MIP was synthesised using a constant molar ratio of template:cross-linker:monomer (Cre:Al^{3+}:TEOS) at 1:5:5. 99

Figure 4.15 Cre-extraction cycle of MIP using different eluents. Note: MIP was synthesised using a constant molar ratio of template:cross-linker:monomer (Cre:Al^{3+}:TEOS) at 1:5:5. 100

Figure 4.16 Adsorbed amounts of Cre in methanol diluent by MIP and NIP extracted using different eluents. Note: MIP and NIP were synthesised using constant molar ratios of template:cross-linker:monomer (Cre:Al^{3+}:TEOS) at 1:5:5 and 0:5:5, respectively. 105

Figure 4.17 Adsorbed amounts of Cre by MIP and NIP and imprinting factors (α) under different conditions. Note: MIP and NIP were synthesised using constant molar ratios of template:cross-linker:monomer (Cre:Al^{3+}:TEOS) at 1:5:5 and 0:5:5, respectively. 109

Figure 4.18 Adsorbate-solvent interactions of (A) Cre-water and (B) Cre-alcohol. 110

Figure 4.19 Optimised conformations of (A) Cre, (B) Cr, (C) *N*-hyd, (D) 2-pyr, (E) Al^{3+} and (F) hydrolysed TEOS. 113

Figure 4.20 Theoretical intermolecular interactions of Cre with Al^{3+}. Note: Arrow indicates the electron shift. 116

Figure 4.21 Theoretical intermolecular interactions of Cre with hydrolysed TEOS. Note: Arrow indicates the electron shift. 117

Figure 4.22 Theoretical intermolecular interactions of Al^{3+} with hydrolysed TEOS. Note: Arrow indicates the electron shift. 118

Figure 4.23 Overall intermolecular interactions of MIP. Note: Arrow indicates the electron shift. 119

Figure 4.24 Molecular electrostatic potential (MEP) of MIP at (A) low (Al^{3+} molarity = 2), (B) optimum (Al^{3+} molarity = 5) and (C) excess (Al^{3+} molarity = 10) molarity of Al^{3+}. Note: The molar ratio of template:monomer (Cre:TEOS) was kept constant at 1:5 (MIP). Green and pink surface areas correspond to positive and negative charges, respectively. 122

Figure 4.25 Adsorption capacities of MIP for Cre, Cr, *N*-hyd and 2-pyr at (A) low (*ca.* 15 mg L^{-1}) and (B) high concentrations (*ca.* 100 mg L^{-1}), respectively. Note: MIP was synthesised using a constant molar ratio of template:cross-linker:monomer (Cre:Al^{3+}:TEOS) at 1:5:5. 124

Figure 4.26 Competitive adsorption by MIP in binary mixture solutions. Note: MIP was synthesised using a constant molar ratio of template:cross-linker:monomer (Cre:Al^{3+}:TEOS) at 1:5:5. 128

Figure 4.27 The peak current variations of different film electrodes in methanol (blank adsorption) at 0.7 V. 133

Figure 4.28 Schematic illustration of (A) CE-MIP and (B) CE-NIP film electrodes. 134

Figure 4.29 Cyclic voltammograms of CE-MIP and CE-NIP film electrodes at *ca.* 15 mg L^{-1} of Cre at 0.7 V. 135

Figure 4.30 The peak current variations of CE-MIP and CE-NIP film electrodes and imprinting factors (α) for Cre and Cr at (A) low (*ca.* 15 mg L^{-1}) and (B) high concentrations (*ca.* 150 mg L^{-1}), respectively, at 0.7 V. 136

Figure 4.31 The peak current variations of the CE-MIP film electrode for Cre and Cr at different concentrations at 0.7 V. 138

LIST OF PLATES

		Page
Plate 4.1	Field emission scanning electron microscopy (FESEM) images (magnification of 20 000×) of MIP and NIP using different types of cross-linkers. Note: MIP and NIP were synthesised using constant molar ratios of template:cross-linker:monomer (Cre:AMPS/Al3+:TEOS) at 1:5:5 (MIP) and 0:5:5 (NIP), respectively.	75
Plate 4.2	Images and change of thickness (Δt_c) of MIP- and NIP-coated electrodes with additives (MTEOS and PTEOS) and without additive at synthesis temperature of 30 °C. Note: $MIP_{additive}$ and $NIP_{additive}$ were synthesised using constant molar ratios of template:cross-linker:monomer:additives (Cre:Al^{3+}:TEOS:MTEOS: PTEOS) at 1:5:5:0.5:0.5 and 0:5:5:0.5:0.5, respectively. MIP and NIP were synthesised using constant molar ratios of Cre:Al^{3+}:TEOS at 1:5:5 and 0:5:5, respectively.	131

LIST OF ABBREVATIONS

2-pyr	2-pyrrolidinone
4-vpy	4-vinylpyridine
AIBN	Azo *N*-*N*'-bis isobutyronitrile
AM	Ally mercaptan
AMPS	2-acrylamido-2-methylpropane-sulfonic acid
BAP	Benzo[α]pyrene
BET	Brunauer-Emmet-Teller
BJH	Barrett-Joyner-Halenda
BSA	Bovine serum albumin
CE	Carbon electrode
CLM	Cross-linking monomer
Cr	Creatine
Cre	Creatinine
DI	Deionised
DVB	Divinylbenzene
EDS	Energy dispersive spectroscopy
EGGE	Ethylene glycol diglycidyl ether
ELISA	Enzyme-linked immunosorbent assay
EPI	Epichlorohydrin
FESEM	Field emission scanning electron microscope
FITC	Fluorescein isothiocyanate isomer I
FTIR	Fourier transform infrared spectroscopy
GCE	Glassy carbon electrode

HCl	Hydrochloric acid
HPLC	High-performance liquid chromatography
MAA	Methacrylic acid
MEP	Molecular electrostatic potential
MIP	Molecularly imprinted polymer
MIP/GCE	MIP modified electrode
MTEOS	Methyltriethoxysilane
N-hyd	*N*-hydroxysuccinimide
NIP	Non-imprinted polymer
NMP	1-methyl-2-pyrrolidone
NMR	Nuclear magnetic resonance
OPA	*O*-phthalic dialdehyde
PM3	Parameterised model number 3
PMAA/SiO_2	Polymethacrylic acid/silica gel
PTEOS	Phenyltriethoxysilane
PVC	Polyvinyl chloride
TEOS	Tetraethoxysilane
TGA	Thermal gravimetric analysis
tt-MA	*Trans,trans*-muconic acid
UAEE	Urocanic acid ethyl ester
β-CD	β-cyclodextrin

LIST OF SYMBOLS

$[Cre]$	Initial concentration of Cre solution (mg L^{-1})
$\Delta Cre_{MIP-NIP}$	Shape factor
ΔE	Interaction energies (kcal mol^{-1})
ΔG^o	Change of Gibb's free energy (kJ mol^{-1})
ΔH^o	Enthalpy change (kJ mol^{-1})
ΔS^o	Entropy change (J mol^{-1} K^{-1})
Δt_c	Change of thickness (mm)
$\Delta \delta$	Change of partial charges
$1/n$	Measure of adsorption intensity or surface heterogeneity
A_e	Equilibrium concentration of analogue (mg L^{-1})
A_o	Initial concentration of analogue (mg L^{-1})
A_T	Temkin isotherm equilibrium binding constant (L g^{-1} polymer)
B_{DR}	Dubinin-Radushkevich isotherm constant (mol^2 J^{-2})
b_T	Temkin isotherm constant
B_T	Temkin isotherm constant related to heat of adsorption (J mol^{-1})
C_a	Equilibrium Cre concentration on MIP or NIP (mg L^{-1})
C_e	Equilibrium Cre concentration (mg L^{-1})
C_o	Initial Cre concentration (mg L^{-1})
C_t	Residual Cre concentrations at time t (mg L^{-1})
E	Mean free energy (kJ mol^{-1})
$E_{Analogue}$	Energy of free analogue (kcal mol^{-1})
$E_{Complex}$	Energy of the MIP complex (kcal mol^{-1})
E_{Cre}	Energy of free Cre (kcal mol^{-1})

$E_{Cross\text{-}linker}$	Energy of free cross-linker (kcal mol^{-1})
$E_{Monomer}$	Energy of free monomer (kcal mol^{-1})
h	Initial adsorption rate (mg g^{-1} polymer min^{-1})
I	Peak current variation (μA)
K	Diffusion rate constant
k_1	Rate constants of pseudo-first-order equation (min^{-1})
k_2	Rate constants of pseudo-second-order equation (g polymer mg^{-1} min^{-1})
k_{Binary}	Competitive selectivity coefficient
K_d	Equilibrium dissociation constant (mg L^{-1})
K_D	Linear adsorption distribution coefficient
K_F	Freundlich constant (mg g^{-1} polymer)
k_{Ideal}	Ideal selectivity coefficient
K_L	Langmuir constant (L mg^{-1})
n	Number of cross-linker or monomer in the MIP complex
P/P_o	Relative pressure
Q	Adsorption capacity (mg g^{-1} polymer)
Q_e	Adsorption capacity at equilibrium (mg g^{-1} polymer)
Q_m	Theoretical isotherm saturation capacity (mg g^{-1} polymer)
Q_{max}	Apparent maximum number of binding sites (mg g^{-1} polymer)
Q_{MIP}	Adsorption capacity of MIP (mg g^{-1} MIP)
Q_{NIP}	Adsorption capacity of MIP (mg g^{-1} NIP)
Q_o	Maximum adsorption capacity (mg g^{-1} polymer)
Q_t	Adsorption capacity at time t (mg g^{-1} polymer)
R	Universal gas constant (J mol^{-1} K^{-1})
R'	Liquid film diffusion constant

R^2	Linear regression correlation coefficients
R_L	Favourability of Langmuir isotherm
t	Time (s)
T	Absolute temperature (K)
$t_{1/2}$	Half-adsorption time (min)
t_c	Thickness (mm)
t_s	Statistical thickness (Å)
V	Volume of solution (L)
W	Mass of MIP or NIP (g)
W_f	Resultant dried mass of MIP (g)
W_o	Mass of fresh MIP (in gel form) (g)
α	Imprinting factor
$\Sigma Cre_{equilibrium}$	Total amount of Cre at equilibrium (mg)

PEMAHAMAN MIKROSKOP TEKAPAN MOLEKUL MATRIK SOL-GEL UNTUK BIOSENSOR PENGECAMAN KREATININ

ABSTRAK

Polimer tekapan molekul (MIP) telah menarik perhatian yang besar dalam sistem pengiktirafan biomimetik disebabkan oleh pengiktirafan molekul secara terpilih terhadap sebarang sasaran yang berminat. Memandangkan toleransi terma, kimia dan mekanikal yang luar biasa di bawah pelbagai keadaan, MIP telah menjadi salah satu peranti "pintar" yang berpotensi dalam aplikasi bioperubatan, seperti industri farmaseutikal, analisis klinikal dan pengesanan dalam *vivo* atau dalam *vitro*. Walau bagaimanapun, salah satu isu utama yang mencabar MIP adalah kesesuaian konformasional MIP. Berbanding dengan diagnostik bioperubatan konvensional, seperti ujian imunosorben berkaitan dengan enzim (ELISA), kesukaran dalam mengawal kekhususan bentuk atau "memori molekul" dalam MIP untuk penekapan molekul yang terbaik telah membatasi potensi MIP sebagai alat pengesanan. Sebenarnya, integriti morfologi yang optimum merupakan faktor utama untuk menentukan kejayaan aktiviti pengesanan oleh MIP. Oleh itu, kajian ini bertujuan untuk menjelaskan konsep utama bagi penekapan molekul, terutamanya mekanisme asas MIP di sebalik penerangan biasa terhadap pengiktirafan molekul. Pertama, ilmu kimia "host-guest" dikaji secara terperinci, dari segi interaksi-interaksi antara molekul untuk menjelaskan tingkah laku pengiktirafan molekul sasaran (templat), kreatinin (Cre) oleh MIP. Cre ialah satu produk akhir degradasi yang spontan dan bukan enzim bagi kreatin (Cr) atau metabolisme fosfokreatin dalam vertebrat, yang berfungsi sebagai penanda bio yang boleh dipercayai untuk menilai disfungsi buah pinggang,

tiroid dan otot. Dalam kajian ini, Cre ditekapkan melalui perkongsian elektron tunggal dari atom nitrogen (N) bagi Cre dan atom oksigen (O) bagi matrik sol-gel kepada asid Lewis Al^{3+}. Untuk memperkukuhkan lagi ketegaran memori bentuk MIP, Cre telah disingkirkan dari polimer dengan satu siri bahan eluat melalui kaedah fizikal supaya meninggalkan satu rangka dengan sterik dan fungsi kesalinglengkapan yang pelbagai terhadap Cre. Merujuk kepada data eksperimen, ingatan molekul bagi Cre yang terbaik telah dicapai dengan menggunakan metanol dan MIP berjaya memperolehi pengambilan Cre secara terpilih sebanyak 19.48 ± 0.64 mg g^{-1} MIP walaupun dalam kewujudan pengganggu analog yang berfungsi sama, seperti Cr, dan/atau berstruktur sama, seperti *N*-hidroxisuccinimida (*N*-hyd) dan 2-pyrrolidinone (2-pyr), dengan pekali terpilih yang kompetitif masing-masing sebanyak 3.01 ± 1.11, 3.75 ± 0.57 dan 5.24 ± 4.59. Dengan ramalan sifat kimia yang berkuasa dan boleh dipercayai untuk sistem biomolekul, sistem MIP telah dirasionalkan dengan bantuan alat linguistik kimia, iaitu HyperChem berdasarkan kaedah mekanik kuantum separa-empirikal *Parameterised Model* nombor 3 (PM3). Pemodelan molekul ini telah mencapai persetujuan yang bagus antara pengiraan teori dan data empirikal, yang mana melanjutkan kesahihan bagi penapisan pengiraan untuk sistem MIP dalam pendekatan bebas daripada eksperimen. Akhirnya, MIP telah disalutkan secara filem pada elektrod karbon sebagai biosensor bersepadu yang menterjemahkan tindak balas kimia dari Cre ke tindak balas elektroanalitik, mencapai kira-kira 1.4 µA. Semasa persampelan kencing tiruan, elektrod filem Cre-MIP mengatasi prestasi dalam analisis campuran binari, mencapai binari empirikal *I* sebanyak 1.4823 ± 0.0267 µA untuk nisbah molar Cre:Cr pada 80:20. Penekapan molekul telah sekali lagi membuktikan kelayakannya dalam biosensor Cre-MIP melalui prestasi pengesanan elektrokimia. Oleh itu, kajian

ini telah menghasilkan reka bentuk praktikal MIP untuk pengesanan disfungsi buah pinggang dengan ujian titik penjagaan bagi Cre.

MICROSCOPIC INSIGHT OF MOLECULARLY IMPRINTED SOL-GEL MATRIX FOR CREATININE-RECOGNISED BIOSENSOR

ABSTRACT

Molecularly imprinted polymer (MIP) is important in biomimetic recognition systems owing to its selective molecular recognition towards any guest of interest. Considering the exceptional thermal, chemical and mechanical tolerance under a wide variety of conditions, MIP has been one of the potential "smart" devices in biomedical applications, such as pharmaceutical industry, clinical analysis and *in vivo* or *in vitro* sensing. However, one of the major issues that challenges MIP lies on the conformational adaptability of MIP. As compared to the conventional biomedical diagnostics, such as enzyme-linked immunosorbent assay (ELISA), the difficulties in controlling the shape-specificity or molecular memory within MIP for the best molecular fitting has restricted the potential of MIP as a sensing tool. In fact, the optimal morphological integrity is the key factor to define the successful sensing activity by MIP. As such, the present study intends to furnish the key concepts of molecular imprinting, particularly the underlying mechanisms of MIP beyond the usual description of molecular recognition. First, the host-guest chemistry is studied in detail, in terms of intermolecular interactions, to elucidate the recognition behaviour of target molecule (template), creatinine (Cre) by MIP. Cre is a spontaneous and non-enzymatic degradation end product of creatine (Cr) or phosphocreatine metabolism in vertebrates, which serves as a reliable biomarker in assessing renal, thyroid and muscular dysfunction. In this study, the imprinting of Cre is ascertained via sharing of lone pair electrons from nitrogen (N) atom of Cre and oxygen (O) atoms of the sol-gel

matrix, respectively, to the Al^{3+} Lewis acid. To further fortify the shape memory stiffness of MIP, Cre is removed from the organised architecture by a series of eluents via physical means, leaving behind a binding framework with varying steric and functional complementarity to Cre. Referring to the experimental data, the best Cre-molecular memory is imparted by methanol eluent, making MIP capable of selective uptake of Cre up to 19.48 ± 0.64 mg g^{-1} MIP even in the presence of functionally alike, i.e., Cr, and/or structurally alike interfering analogues, i.e., *N*-hydroxysuccinimide (*N*-hyd) and 2-pyrrolidinone (2-pyr), by competitive selectivity coefficients of 3.01 ± 1.11, 3.75 ± 0.57 and 5.24 ± 4.59, respectively. Coupled with the powerful and reliable prediction of chemical properties for biomolecular system, the MIP system is rationalised with the aid of a computational chemistry tool, HyperChem based on the Parameterised Model number 3 (PM3) semi-empirical quantum mechanics method. The molecular modelling has come up with a good agreement between the theoretical computations and the empirical data, which extends the validity of computational screening in the MIP system in an experimental-free approach. Finally, the MIP is film-coated on carbon electrode as an integrated biosensor that translates the chemical response from Cre into an electroanalytical response, reaching *ca.* 1.4 µA. During artificial urinary sampling, the Cre-MIP film electrode outperforms in the binary mixture analysis, attaining an empirical binary *I* at 1.4823 ± 0.0267 µA for Cre:Cr at 80:20 molar ratio. It is noteworthy that molecular imprinting has once again proven its feasibility in Cre-MIP biosensor through the electrochemical sensing performance. Henceforth, this study has come up with a practical design of MIP for the detection of renal dysfunction by point-of-care testing for Cre.

CHAPTER ONE

INTRODUCTION

1.1 Molecularly Imprinted Polymer (MIP)

Molecular imprinting is defined as the creation of selective recognition cavities for the target molecule (template) in a polymer matrix by judiciously selected monomers, with the optional aid of a cross-linking agent, as schematically depicted in Figure 1.1. In essence, the template guides the positioning and orientation of the building blocks in a manner that contours its structural and chemical character via a self-assembly mechanism (Ye and Mosbach, 2008, Lofgreen and Ozin, 2014) based on the "molecular key and lock" principle (Fischer, 1894).

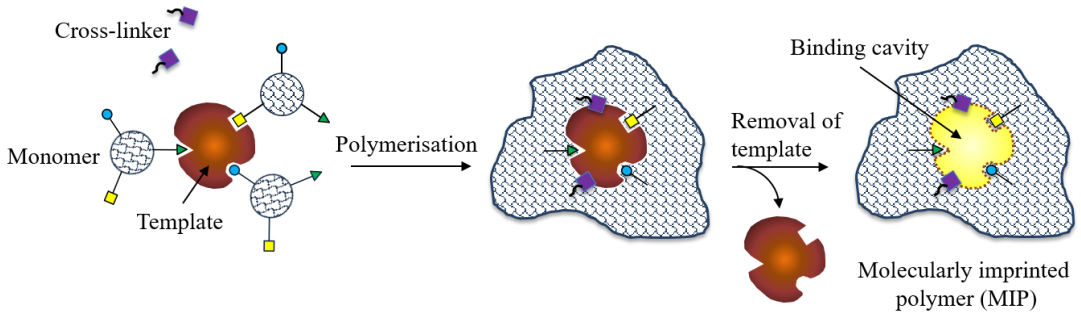

Figure 1.1: Schematic illustration of molecular imprinting.

In molecular imprinting, the template could be ranging from atomic level, including ion, to complex macromolecular assembly, such as proteins and cells (Haupt and Mosbach, 2000, Ng and Narayanaswamy, 2010). Firstly, solvent or porogen will be used as the medium of polymerisation to stabilise the interactions between the template-monomer complexes (Cummins et al., 2005). The rigidity of the polymer network is imparted by the inclusion of a highly cross-linked polymeric structure,

which fixes the template-monomer complexes into the spatial arrangement. Generally, the imprinting process involves the polymerisation of monomer either covalently or non-covalently in the presence of template (Dickert and Hayden, 1999). In covalent imprinting, strong reversible covalent bonds are formed between the polymerisable monomer and the template (Al-Kindy et al., 2000). These covalent arrangements include boronate esters, Schiff bases or ketal. Meanwhile, non-covalent imprinting refers to a self-assembly of the monomeric species around the template by weak intermolecular forces, such as π-π and hydrogen bonding, Van der Waals forces, electrostatic, ion or hydrophobic interaction and metal coordination (Al-Kindy et al., 2000, Vasapollo et al., 2011). The non-covalent imprinting is favoured because of its flexibility on the selections of monomer and template as well as simpler preparation protocol as compared to the covalent approach. Moreover, the subsequent procedure to remove the template is straightforward for the non-covalent approach. The template removal involves a simple diffusion mechanism whereby a polar or acidic eluent is sufficient to overcome the non-covalent interactions between the template and MIP (Bergmann and Peppas, 2008). Therefore, it is not surprising that the non-covalent approach is broadly applied in the preparation of MIP.

Upon completion of the polymerisation, the template is removed by physical means, leaving behind a binding framework (or void cavities within the polymer matrix) with steric and functional complementary to the template (Chen et al., 2016). By this way, the molecular memory is induced, making the organised architecture capable of selective uptake of the target analyte from a pool of closely related compounds (Chen et al., 2011). This tailor-made mimic for the analyte of interest has made MIP amenable for a diversity of essential analytical applications, especially in chemical/biological sensing (Cieplak et al., 2015, Smolinska-Kempisty et al., 2017).

MIP is able to mimic the biological activity of natural counterparts (Vlatakis et al., 1993, Piletsky et al., 2000b) on par, such as antibody-antigen system, by virtue of high selectivity and affinity (Scognamiglio et al., 2015). Furthermore, in contrast to biological system (Table 1.1), MIP is superior against enzymatic degradation and extreme environments, such as in acids or bases, in organic solvents, or at elevated temperatures and pressures, due to their excellent thermal, chemical and mechanical tolerance (Vasapollo et al., 2011, Dima et al., 2013, Tallawi et al., 2015). Coupled with the advantages of time and cost-effectiveness, in terms of simple synthesis procedure and high yield of regeneration (Bedwell and Whitcombe, 2015), MIP is exceptionally appealing to researchers in a new generation of biomedical diagnostics. In addition, the storage life of MIP can be very high, keeping the recognition capacity up to several years without degradation. Special sample pre-treatments, such as purification, are excluded (Ghasemi and Nematollahzadeh, 2018) and MIP is often employed rather just at ambient conditions. As such, the involvement of live samples which is often necessary at any stage of the preparation of immunoassay has been avoided (Kriz et al., 1997, Lavignac et al., 2004) because MIP is a synthetic material from chemical building blocks. In other words, from the practical, ethical and economical points of view, MIP has reaped the benefits, which make them socially acceptable for use in various applications.

With continued rapid progress in polymer chemistry and materials science, molecular imprinting has opened the route for MIP to serve as a selective medium in capturing the analytes of environmental, medical and industrial interest.

Table 1.1: Comparison of MIP and natural biological receptor (Haupt and Mosbach, 2000, Lavignac et al., 2004, Sellergren and Allender, 2005, Vasapollo et al., 2011, Bedwell and Whitcombe, 2015).

	MIP	Biological receptor
Structural properties	Synthetic; no use of animals	Biological production involving live samples
Preparation	Simple and short synthesis time; large scale production is allowed	Complex and time consuming; limited to large scale production
Target molecules	Any feasible compound	Restricted access to important analytes
Binding site properties	Heterogeneous binding sites, leading to affinity distributions with different adsorption energies; well represented by Langmuir-Freundlich or Freundlich isotherm generally	Homogeneous binding sites, showing uniform affinity with similar adsorption energy; fitted well to the Langmuir isotherm generally
Stability	High stability; can be used in both aqueous and organic media	Low stability; can work only under aqueous media and specific temperature
Storage life	No pre-treatment; can be kept up to several years without degradation	Lyophilisation (or freeze drying) is required; prone to denaturation upon long period storage
Cost	Inexpensive (depends on monomer selection); can be regenerated	High price of receptors; non-regenerable
Reproducibility	Controllable from batch to batch	Partially controllable; can be very selective
Micromachining technology compatibility	Highly compatible	Poor compatibility
Immobilisation for sensing application	Do not require; can be used directly	Require additional steps

1.2 Sol-Gel Approach

Taking into account the evolution in MIP preparation protocol, sol-gel polymerisation has drawn much attention of researchers globally in recent decades, particularly in the discipline of materials science. Sol-gel materials are commonly conferred with outstanding chemical inertness, high purity, rigidity, controlled porosity (Mujahid et al., 2010) and optical transparency (down to 250 nm) (Jerónimo et al., 2007), conferring them the suitability as optical (Li et al., 2011, Karfa et al., 2016) and bio-sensing devices (Graham et al., 2002, Karaseva et al., 2016, Zhang et al., 2016a).

Sol-gel technique is the most feasible and versatile alternative for the synthesis of porous polymeric materials possessing unique properties at low temperature (Mujahid et al., 2010) and under mild chemical conditions (Lin and Brown, 1997). In a sol-gel process, hydrolysis of alkoxide precursors precedes polycondensation reaction of metal alkoxides during the transition of a liquid "sol" into solid "gel" (Brinker, 1990). The polycondensation reaction increases the viscosity of the system progressively while the "gel" will interconnect with each other until the formation of a strong and dense glass-like structure besides some other by-products (water or alcohols)(Basabe-Desmonts et al., 2007), which are eliminable by drying or heat treatment. The two-step hydrolysis-condensation reactions during the course of gel formation could be described as:

Hydrolysis:

$$\mathrm{M(OR)_n + nH_2O \rightarrow M(OH)_n + nR(OH)} \qquad (1.1)$$

Condensation:

$$pM(OH)_n \rightarrow pMO_{n/2} + (pn/2)H_2O \quad (1.2)$$

where M is a network-forming element, e.g., Si, Ti, etc. and R refers to alkyl radical.

The resulted sol-gel structure can be further processed to a variety of shapes embrace thin films, gels and ceramics (Brinker, 1990), which allows different configurations of sensing approach based on its final applications (Schulz-Ekloff et al., 2002). The overall molecular imprinting of template within the sol-gel network is schematically represented by the scheme of Figure 1.2.

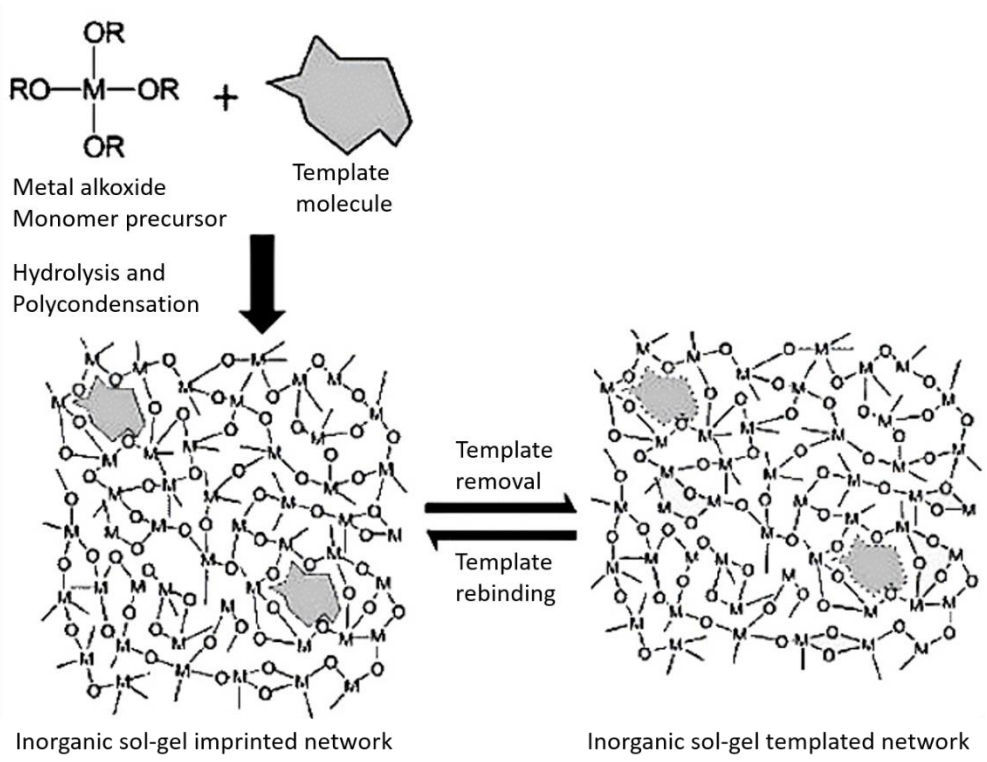

Figure 1.2: Schematic illustration of molecular imprinting via sol-gel process; M is a network-forming element, e.g., Si, Ti, etc.; R refers to an alkyl radical (Lee and Kunitake, 2013).

1.3 Creatinine

Creatinine (Cre) is a spontaneous and non-enzymatic degradation end product of creatine (Cr) or phosphocreatine metabolism in vertebrates (Wyss and Kaddurah-Daouk, 2000) whereby Cr, a by-product of amino acid metabolism, is the energy source for the muscular tissue. Cr is carried in the blood serum or plasma in its dehydrogenated form, Cre (Killard and Smyth, 2000). In other words, Cre is continuously produced in the human body, which is then expelled as urinary discharge. Endogenous Cre production is constant as long as the muscle mass remains constant (Fischbach and Dunning, 2009). Considering its relatively constant concentration in blood serum or plasma and urinary excretion from dietary change, Cre level serves as a reliable biomarker in assessing renal, thyroid and muscular dysfunction (Soldatkin et al., 2002). The normal clinical ranges of Cre in human blood serum or plasma and urine are 44 – 106 µM (5.8 – 14 µg mL^{-1}) (Killard and Smyth, 2000) and 2.5 – 23 mM (0.28–2.59 mg mL^{-1}) (Arndt, 2009), respectively. For routine clinical samples of blood serum or plasma, levels above 140 µM (16 µg mL^{-1}) require clinical investigation and levels over 530 µM (60 µg mL^{-1}) indicate severe renal impairment (Mădăraş and Buck, 1996). In addition, Cre concentration can also be employed as a standardisation tool for quantifying therapeutic drugs, illicit drugs and xenobiotics in urine (Liotta et al., 2009).

The most common method adopted in measurement of Cre concentration is Jaffé's reaction, a colorimetric method proposed in 1886. According to Jaffé (Tsai and Syu, 2005a, Tsai and Syu, 2011), the active methylene group of Cre will react with the alkaline sodium picrate to form a red-yellow complex of Janovsky (Debus et al., 2015). This coloured complex is then detected by a spectrophotometric analyser. This method, however, is seriously prone to interference, such as blood metabolites (e.g., bilirubin,

urea and dopamine), and thus loses the specificity easily (Weber and van Zanten, 1991, Osaka et al., 2000, Wyss and Kaddurah-Daouk, 2000). Owing to the simplicity, stability, time and cost-effectiveness of biosensor system, the development of non-enzymatic Cre-based biosensor is proposed for clinical analysis.

1.4 Problem Statement

In modern healthcare, many diagnostic techniques are available, such as chromatography in laboratory tests, enzyme-linked immunosorbent assay (ELISA) and imaging techniques (e.g., radiology and ultrasound examination). Undoubtedly, these *in vitro* diagnostics guarantee the outcomes with remarkable accuracy and sensitivity (Wang et al., 2014, Kong et al., 2015). However, these conventional immunoassays are typically time-consuming, susceptive to high background noise and requiring advance equipment or instruments (Mire-Sluis et al., 2004, Garcia-Cortes et al., 2016, Mou and Jiang, 2017), such as high-performance liquid chromatography (HPLC). In the field of biomedical diagnostics, the major limitations associated with conventional diagnostic techniques are their time ineffectiveness as well as the involvement of complex procedures (Kong et al., 2015, Yamada et al., 2017). Henceforth, there has been of great interest in developing low-cost techniques for accurate and rapid diagnostics of various diseases, especially a sensing tool with high selective ability. MIP is hence envisaged as a more versatile and promising substitution to the conventional bio-sensing device.

Despite the powerfulness of molecular imprinting, MIP faces big challenges on the conformational integrity, especially the difficulties to control the shape-specificity or molecular memory of polymer matrix to biomolecules. Indeed, the

optimal conformational integrity of MIP in creating the synthetic receptor is the key factor to determine the effectiveness of selective sensing activities. Unfortunately, the conformational adaptability of the linear polymer is limited; hence, the template molecule and the surrounding polymer chains are not able to produce the best molecular fitting in most scenarios. With continued rapid progress in polymer chemistry, the underlying principles of MIP should have been disclosed deeper and better understood to give way to MIP for various applications.

In materials science, the intermolecular interactions of building blocks, e.g., template, functional monomer, cross-linker, are of predominant significance in visualising the structural arrangement of MIP. Yet, the chemical interactions of MIP are hardly interpretable through typical characterisations, such as Fourier-transform infrared spectroscopy (FTIR) and nuclear magnetic resonance (NMR) spectroscopy. To better understand the host-guest chemistry of the MIP complex, molecular dynamic modelling strategies are often employed to obtain the basic interpretations, such as charge distribution and binding score. Such computational chemistry tools, such as *ab initio* method, density functional method, molecular dynamics method, etc., are capable of predicting molecular properties including stable conformations, vibrational frequencies of atoms, molecules and reactive systems. These theoretical predictions can thus serve as a guideline in the selection of monomers and/or cross-linkers for a target analyte.

As far as MIP is concerned, the physical appearance has been another challenging aspect whereby the powdered MIP is relatively difficult to handle during bio-sensing applications. Owing to the tendency of mass loss, the evaluation of powdered MIP, especially which lies within the nano range, is of high challenges. Considering the feasibility of transducer membrane in membrane separation,

polyelectrolytes are usually applied to immobilise the powdered MIP onto a supporting thin film. This integration has made the application of biosensor simple by dipping it into the analytes for analysis.

Under the National Key Economic Area, the healthcare ecosystem (with three sub-sectors of pharmaceuticals and biotechnology, medical technology and health services) has always been credited as the most crucial segment in the overall Malaysian economy. The development of MIP is definitely in consensus with the aim of government to leverage the nation's manufacturing benefits and on-going research efforts, especially diagnostic test kits, so as to give a better-quality care for all the Malaysians.

1.5 Research Objectives

The principal objective of this study is to synthesise Cre-imprinted sol-gel matrix for the Cre-based biosensor. The present study aims at the following objectives:

1. To synthesise MIP as selective stationary phase for the detection of Cre in assessing the non-enzymatic Cre-based biosensor.
2. To evaluate the rigidity of the polymer structure to ensure the cavities shape is retained after template removal.
3. To model the morphological effect of different polymerisation conditions in affecting the MIP recognition sites using HyperChem.
4. To ascertain the binding selectivity of MIP through chromatographic separation for the Cre analogues.

5. To integrate MIP onto carbon electrode as an electrochemical Cre-MIP biosensor and evaluate its specificity and sensitivity towards recognition of Cre.

1.6 Scope of Study

In this study, MIP is prepared via sol-gel approach to selectively recognise Cre template for the detection of renal dysfunction. To optimise the conformational integrity of MIP, the nature of cross-linker, cross-linking density and monomer concentration are manipulated in detail. Different natures of cross-linkers; organic 2-acrylamido-2-methylpropane-sulfonic acid (AMPS) and inorganic aluminium chloride hexahydrate ($AlCl_3 \cdot 6H_2O$), are studied and compared to figure out the intermolecular interactions and strength of the chemical bonds between the Cre template and the monomer, tetraethoxysilane (TEOS). Investigations on the cross-linking degree from molar ratio of 0 to 10 and the monomer formulation from molar ratio of 5 to 25 are done to form a confined matrix with the best molecular fitting for Cre. The MIP and non-imprinted polymer (NIP) systems are characterised via Fourier transform infrared spectroscopy (FTIR), thermal gravimetric analysis (TGA), field emission scanning electron microscope (FESEM), nitrogen adsorption-desorption analysis and energy dispersive spectroscopy (EDS) to ensure the effectiveness of Cre-imprinting.

To effectively deepen the theoretical understanding on the adsorption phenomenon of Cre by MIP, based on the optimum structure of MIP, the binding mechanisms are elucidated via adsorption kinetics to describe the rate-controlling step of Cre. The binding characteristics of Cre by MIP by the mean of chemical, physical or physicochemical properties are also interpreted through Langmuir, Freundlich Temkin and Dubinin-Radushkevich isotherm models. In addition, Scatchard analysis

is used to define the diversity of Cre-recognition sites from the aspect of affinity constant. For the determination of temperature dependence of Cre-adsorption rate by MIP, thermodynamic study is conducted.

Subsequently, the elution effect on MIP is further examined by employing a series of eluents range from very polar (i.e., deionised (DI) water) to polar (i.e., methanol and propanol) to non-polar (i.e., chloroform) to explore a suitable eluent that imposes the least possible shape rupture impact to the sol-gel host matrix while maintaining the optimal molecular recognition cavities after template removal. By optimising the shape complementarity of MIP, the solvation effect is testified in detail to inspect the relationships between the Cre template, MIP system and solvents.

With the aid of HyperChem, a molecularly dynamic simulation tool, the MIP system is rationalised, in terms of the Mulliken atomic charge, intermolecular interaction energies (ΔE) and molecular electrostatic potential, using Parameterised Model number 3 (PM3) semi-empirical quantum mechanics method to correlate the experimental data with the theoretical computations.

To fulfill state of the art of MIP system, the recognition capability of MIP for Cre from its interfering analogues of similar, or different, chemical structure, i.e., Cr, *N*-hydroxysuccinimide (*N*-hyd) and 2-pyrrolidinone (2-pyr), must be compromised. Both the competitive and non-competitive interference analyses are performed to assess the discrimination ability of MIP towards Cre for a fixed area of binding sites. The experimental data are measured by a HPLC. As well, the MIP system is simulated by HyperChem to compare and justify again the selective recognition of MIP for Cre.

Lastly, the MIP is film-coated onto a carbon electrode (CE) as an integrated Cre-MIP biosensor. Coupled with the three-electrode system, cyclic voltammetry is

performed by a three-electrode potentiostat system to prove the analytical performance of Cre-MIP biosensor qualitatively and quantitatively.

1.7 Thesis Organisation

This thesis is organised into five chapters. A brief description on molecular imprinting, particularly via sol-gel technology, and the target analyte, Cre is overviewed in Chapter One to provide a holistic view on the background of this study. The problem statement reveals the current scenario of imprinting technology that restricts the development of MIP in sensing. As such, the research objectives and scope of study are elucidated accordingly to address the issues encountered in molecular imprinting.

A comprehensive review on state of the art and perspectives of molecular imprinting is outlined in Chapter Two. The underlying principles of MIP from preparation stage to biosensor applications are also highlighted using the existing literature. As well, the potential applications of MIP are furnished based on the on-going research in biomedical diagnostics to develop an artificial Cre receptor for the detection of renal dysfunction.

Chapter Three begins with a research flow chart to illustrate the overall outline of current research. The details of materials, experimental procedures, morphological characterisation techniques, imprinting performances and other relevant analyses are reported in a thorough manner.

Chapter Four consists of the core and in-depth discussions based on all the crucial findings obtained throughout the study. In accordance with the research objectives presented in Section 1.5, the structural analysis of MIP is presented from

the aspects of host-guest chemistry and adsorption mechanism. The scientific investigation is then focused on the shape memory stiffness of MIP by evaluating the elution and solvation effects on MIP. The MIP system is then rationalised by HyperChem to validate again the experimental results with theoretical modelling. Subsequently, the selective recognition of MIP for Cre is evaluated to ascertain the role of Cre-shape memory within MIP through non-competitive and competitive selectivity study. This chapter ends with the integration of MIP into electrochemical Cre-based biosensor by scrutinising its specificity and sensitivity.

The findings of this study, which correspond to the research objectives in Section 1.5, are summarised in Chapter Five. Some related considerations and directions are also proposed to direct further investigations in future work.

CHAPTER TWO

LITERATURE REVIEW

2.1 Molecular Imprinting Technology

Molecular imprinting is an attractive technique to substantial research efforts in complementing the quest of biomimetic recognition systems. It is one of the most widely studied advanced systems designed to exhibit high selectivity and affinity for a diversity of essential analytical applications, especially in chemical/biological sensing of environment, industrial and medical interest (Resmini, 2012, Anirudhan and Alexander, 2014, Cieplak et al., 2015, Smolinska-Kempisty et al., 2017, Samah et al., 2018).

2.1.1 Molecular Imprinting Principle

Pioneering work on molecular imprinting has been done extensively through organic methods, which involve either covalent or non-covalent interaction between the template, monomer and/or cross-linker, as illustrated in Figure 2.1.

A

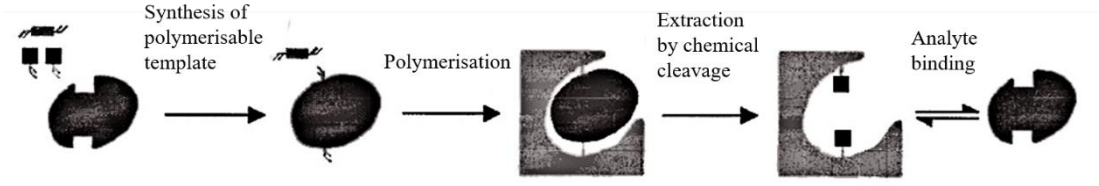

Figure 2.1: Schematic diagram of (A) covalent and (B) non-covalent molecular imprinting approaches (Haupt and Mosbach, 2000).

B

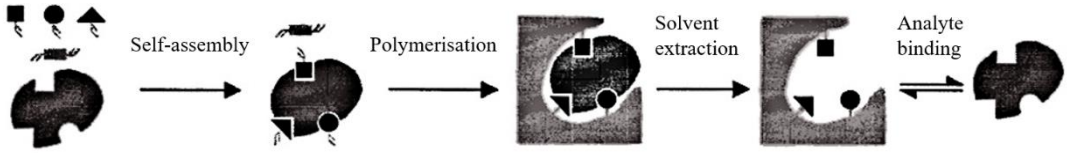

Figure 2.1: Continued.

In covalent or pre-organised imprinting first established by Wulff et al. (1977), strong reversible covalent bonds are formed between the polymerisable monomer and the template molecule. The covalent approach is prevailing in the strong template-monomer interactions, leading to the formation of the rigid imprinted shape cavities whereby the binding sites are highly specific and homogeneous (Al-Kindy et al., 2000). The imprinted shape is reliant on the cleavage of these covalent arrangements (Yan and Ramström, 2005) includes boronate esters, Schiff bases and ketal. However, a reduced reversibility and slower speed of the template removal is noticed. As a rule of thumb, the chemical linkage of the template-monomer complex must be stable under polymerisation conditions (Bergmann and Peppas, 2008), yet this intermolecular interaction ought to be overcome easily to form the selective recognition cavities with induced molecular memory. Unfortunately, it is hardly for most of the covalent bonds to comply these requirements. Consequently, the covalent approach is not as extensively studied as the non-covalent approach.

Arshady and Mosbach (1981) have proven that covalent interactions are not compulsory in molecular imprinting. In non-covalent imprinting, self-assembly of the monomeric species around the template molecule occurs by weak intermolecular forces, such as π-π and hydrogen bonding, Van der Waals forces, electrostatic, ion or hydrophobic interaction and metal coordination (Al-Kindy et al., 2000, Vasapollo et al., 2011, Lee and Kunitake, 2013). The non-covalent approach attracts many concerns due to its simplicity in the formation and dissociation of the template-monomer

complex and the versatility in monomer selection towards the template (Yan and Row, 2006). In other words, the removal of the template is reasonably easier via simple diffusion in which a polar solvent or eluent could have sufficiently overcome the intermolecular forces between the template and the polymer (Bergmann and Peppas, 2008). Moreover, the template rebinding or the selective recognition of the target analyte is facilitated because the formation of covalent bond is exempted (Haupt, 2003). Henceforth, most of the evolvement of molecular imprinting focus in this area, especially in the imprinting of biomolecules that is rather complicated.

2.1.2 Molecular Imprinting Technique

Literally, various imprinting methods have been considered in the preparation of MIP embrace bulk polymerisation (He et al., 2007, Shiraishi et al., 2010), free radical polymerisation (Li et al., 2012a, Yu et al., 2010, Qiu et al., 2015b), graft polymerisation (Sellergren et al., 2002, Anirudhan and Sandeep, 2011), precipitation polymerisation (Stringer et al., 2011, Miura et al., 2013), sol-gel polymerisation (Chang et al., 2009, Tsai and Syu, 2011, Li et al., 2012b, Chen et al., 2013, Zhou et al., 2013, Morais et al., 2017), thermal polymerisation (Bakas et al., 2012, Wu et al., 2017), etc.

2.1.2(a) Bulk Polymerisation

Bulk polymerisation is one of the simplest techniques that require only monomer and monomer-soluble initiators, possibly a chain-transfer agent for molecular weight control (Vasapollo et al., 2011, Carraher, 2017). MIP of high clarity and large molecular weight is produced through this method because the diluent or

dispersing agent is absent in bulk polymerisation. One of the advantages of bulk polymerisation is its high reaction rate, which is interrelated to the high concentration of monomer, resulting in a high polymer yield per volume of reactor and easy polymer recovery (Carraher, 2017).

While bulk polymerisation may offer some benefits as compared to other polymerisation methods, the process is, however difficult to control owing to the fact that it is exothermic in nature (Kent, 2012). Even at low conversion, the viscosity of the system increases rapidly and hence, thermal control is required either via continuous stirring or external cooling (Carraher, 2017). Nevertheless, heat removal is a big concern because of the low thermal conductivity of the polymer and the high viscosity of the polymer in which local hot spots can easily occur, leading to the degradation of polymer quality. Indeed, the thermal build-up can be minimised by conducting the polymerisation at low conversion or in few stages. In a study conducted by He et al. (2007), a quinine-imprinted polymer was prepared by bulk polymerisation under two different initiation methods, namely, thermal polymerisation and photo polymerisation. It was interesting to figure out that the MIP prepared under photo-initiated bulk polymerisation at 15 ºC is only slightly selective towards quinine than that of the thermal-initiated bulk polymerisation at 55 ºC by 5.91 μmol g^{-1}. He et al. (2007) deduced that there was a trade-off between the completeness of polymerisation and the stability of the template-monomer complex, in terms of the strength and structure, in which the former was favoured at high temperature, whereas low temperature was advantageous in the latter.

2.1.2(b) Free-Radical Polymerisation

Commonly employed in the preparation of MIP, free radical polymerisation can be conducted under mild reaction conditions (Cormack and Elorza, 2004, Vasapollo et al., 2011), e.g., temperature below 80 ºC and ambient atmospheric pressure. This synthesis procedure is much tolerant of a diversity of template, monomer and impurities in the system, if any, e.g., water. Generally, a free radical polymerisation is characterised by three distinct steps: (a) initiation, (b) propagation (chain growth) and (c) termination, where the propagation rate is much faster than that of the initiation so as to promote the growth of high molecular weight product in a short period of time (sometimes within seconds) before termination. As an illustrative example in Figure 2.2, the common azo-initiator, azo *N*-*N*'-bis isobutyronitrile (AIBN), can be decomposed either thermally or photochemically to polymerise vinyl monomers, such as methyl methacrylate, to give rise to poly(methyl methacrylate).

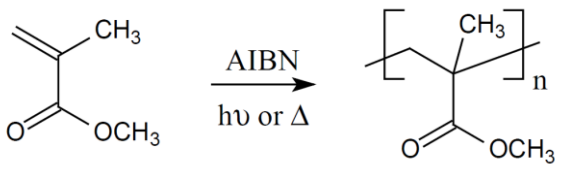

Figure 2.2: Free radical polymerisation of methyl methacrylate into poly(methyl methacrylate).

However, free radical polymerisation hardly offers any degree of control in the molecular size, architecture and number of macromolecules, mainly due to the side reactions, i.e., chain transfer reaction and termination, that affect the growing species throughout the synthesis (Beyazit et al., 2016). Such reactions compete vigorously along with the propagation, causing in dead polymer chains of diverse molecular weights.

2.1.2(c) Sol-Gel Polymerisation

Today, sol-gel method makes any imprinting system virtually possible non-covalently (refer to Section 2.1.1) in a wide range of processing conditions in conjunction with the commercial expansion of sol-gel precursors (Avnir, 1995). In the 1980s, the work of Schmidt on the development of sol-gel composites on an atomic scale was a major kick-start for modern effort in sol-gel materials (Schmidt et al., 1984, Schmidt, 1985).

The sol-gel method uses low molecular weight metal alkoxide as sol-gel precursors, such as tertraalkoxysilanes, to form a highly cross-linked metal oxide according to the overall chemical reaction in Equation (2.1) (Lee and Kunitake, 2013, Lofgreen and Ozin, 2014):

$$n\mathrm{Si(OR)_4} + 2n\mathrm{H_2O} \rightarrow n\mathrm{SiO_2} + 4n\mathrm{ROH} \qquad (2.1)$$

where the metal is represented by Si and R refers to an alkyl group. The transition of the system involves the formation of a colloidal solution or a "sol" by the sol-gel precursors to an integrated network of amorphous material in gel form (Brinker, 1990). In general, the sol-gel processing is aided either by acidic catalyst (pH < 2, such as HCl) or basic catalyst (pH > 2, such as ammonium hydroxide). pH of 2 is the isoelectric point of silica at which the silica carries no net charge and a negligible reaction is expected (Lofgreen and Ozin, 2014). The hydrolysis reaction is much facilitated under acidic medium, whereas the basic catalysis is preferred during the condensation reaction (Ponton et al., 2001). In the acid-catalysed system, a low molecular weight monolith structure is likely to be obtained while a highly cross-linked colloidal particle is created when the basic catalyst is introduced into the sol-gel system. Under the non-

catalysed conditions, the polymerisation may take weeks to reach completion (Lee and Kunitake, 2013).

The sol-gel polymerisation has drawn much scientific attention in the discipline of polymer chemistry and materials science in recent decades. This is attributed to its direct allowance of trace elements, versatility to produce high purity and homogeneous materials, tolerance to the synthesis of variable formats, such as fibres, films, monoliths, reactive ceramic powders, etc (Azimi, 2013). Moreover, the low processing temperatures (within 100 ºC) and in mild chemical conditions (reaction parameters, e.g., pH, water content, reaction rates, etc., are easily manipulated) enable energy saving. Regardless the high precursor cost and prolonged process duration, the potential of sol-gel polymerisation always remain high and attractive that further explorations are putting forward.

2.2 Formulation on Cre-MIP Synthesis

Two key features defining the success of molecular imprinting are: (1) the quality of polymerisation reaction to obtain robust imprinted cavities without shape rupture and (2) the performance of MIP in terms of its binding ability to capture and "lock" the target analyte within the imprinted shape cavities (Yungerman and Srebnik, 2006). Since the pioneering work of Polyakov (1931) in molecular imprinting, substantial progress has been focused on the formulation design of MIP to reflect the gradual maturation on the recognition properties of MIP. There has always been of great interest from the scientific community in understanding the quality and performance of MIP mainly from the aspects of polymerisation conditions (e.g., template-monomer ratio, initiator, porogenic solvent, polymerisation temperature and

pressure, etc.) (Piletska et al., 2009) and nature of the intermolecular interactions on the binding site.

2.2.1 Cross-linker

In molecular imprinting, the choice of cross-linker is crucial in controlling the morphology of the polymer matrix while enhancing the physical stiffness of the imprinted cavities so as to preserve the molecular recognition capacity (Vasapollo et al., 2011). The cross-linker is essential in MIP synthesis to fortify the arrangement of the functional groups of template and monomer for a stable configuration complementary to the imprinted cavities (Al-Kindy et al., 2000).

Prior to the present study, the inorganic aluminium ion (Al^{3+}) has attracted much attention to work as a cross-linker over the past few years for the sake of the structural rigidity with high surface areas and porosities (Ling et al., 2005, Shen et al., 2009, Li et al., 2012b). By the mean of molecular imprinting, a catecholamine receptor was accomplished by (Ling et al., 2005) by interacting the silicate from TEOS with the inorganic Al^{3+} (from aluminium chloride hexahydrate ($AlCl_3 \cdot 6H_2O$)). The relative binding selectivity of MIP to recognise catecholamine was feasibly proven. However, there is a lack of detailed rationale from the aspect of intermolecular interactions in between the core species. Another group of researchers, Shen et al. (2009) have attempted to prepare a photocatalyst for photodegradation of diethyl phthalate, an organic environmental pollutant, by coating a layer of inorganic mesoporous molecularly imprinted silica/Al^{3+} to the surface of TiO_2 nanoparticles. In their study, two receptor sites; framework tetrahedrally coordinated Al^{3+} and non-framework octahedrally coordinated Al^{3+}, were formed on the surface of MIP. The selective

affinity towards diethyl phthalate was achieved at a factor of 3.29 to ensure the mineralisation of the pollutant in a safer approach. Moreover, Li et al. (2012b) also reported the molecularly imprinted silica-alumina gel synthesised from the inorganic precursors of Al^{3+} and TEOS. Based on their empirical data, the Cre-recognition had been effectively enhanced up to 4.80 mg Cre g^{-1} MIP in view of the combined effort of Al^{3+} as Lewis acid sites and covalent bonding between Al^{3+} and TEOS. However, the dominant binding interactions between complementary functional groups of Cre and Al^{3+} remained sceptical.

On the other hand, there are numerous research groups who have attempted to incorporate AMPS precursor on MIP preparation (Piletsky et al., 2000a, Sergeyeva et al., 2001, Anirudhan and Sandeep, 2011, Yang et al., 2012) due to its highly ionisable sulfonate group ($–SO_3H$). For example, Piletsky et al. (2000a) have surface-functionalised the polypropylene membranes with AMPS for specific recognition of desmetryn, a herbicide. Owing to the hydrophilicity and relative rigidity of the binding sites, the template binding specificities were improved remarkably, especially in buffer solutions. Later, Sergeyeva et al. (2001) adopted the similar synthesis protocol to selectively adsorb another herbicide, terbumeton, from the aqueous solution. The binding of terbumeton was assumed to be based on the cation-exchange groups of AMPS. Taking into account the practicability of AMPS on MIP preparation, a bovine serum albumin (BSA) imprinted polymer was formulated from AMPS by Anirudhan and Sandeep (2011). From their observation, the BSA-imprinted polymer exhibited satisfactory affinity and specificity for BSA as a result of multiple hydrogen bonding and electrostatic interaction between BSA and AMPS in the imprinted cavities. By grafting the AMPS on the surface of silanised carbon microspheres, the MIP prepared by Yang et al. (2012) could have specifically recognised dibenzothiophene as efficient

as 46% on the overall adsorption. Considering the AMPS's hydrolytic and thermal stability in a wide range of pH, hydrophilicity and reactivity in altering the chemical properties of the resultant polymer, a thorough insight into the role of AMPS in biomimetic recognition systems attracts researchers' interest, especially from the molecular speculation of chemistry.

2.2.2 Monomer

In order to create a high yield of selective recognition sites and maximise the complementary interactions in the polymer matrix (Al-Kindy et al., 2000), the monomer is normally added in excess relative to the template to favour the formation of the template-monomer complex that is equilibrium-dominated (Vasapollo et al., 2011). As a drawback of the over-equilibrium of the monomer to the template, a heterogeneous distribution of binding sites on MIP is expected because there are numerous configurations of the template-monomer assembly.

Few Cre-templated MIPs have been reported to date. The reported data of adsorbed Cre, percentages of Cre-adsorption, as well as the overall imprinting factors (α) were summarised in Table 2.1. The ratio of the adsorbed amount of Cre by MIP to that by NIP is interpreted as α. A computationally designed highly cross-linked Cre-imprinted polymer was developed by cross-linking of ally mercaptan (AM) and *O*-phthalic dialdehyde (OPA) to urocanic acid ethyl ester (UAEE) in the study carried out by Subrahmanyam et al. (2001). Although the adsorption capacity of MIP was not reported, the computational simulated MIP was able to achieve an imprinting with a factor of 1.44 ± 0.20. On the other hand, a specific receptor of Cre was prepared by Tsai and Syu (2005b) via heated polymerisation of β-cyclodextrin (β-CD) as monomer